A. Maino, G. Janszen, L. Di Landro
Glass/epoxy and Hemp/bio Based Epoxy Composites: Manufacturing and Structural Performances
Polymer Composites, Vol. 40, N. S1, 2019, p. 723-731
doi:10.1002/pc.24973

Glass/epoxy and hemp/bio based epoxy composites: manufacturing and structural performances

Alessandra Maino [a], Gerardus Janszen [b], Luca Di Landro [c],

Politecnico di Milano - Department of Aerospace Science and Technology, Via La Masa 34, 20156 Milano, Italy

[a]alessandra.maino@polimi.it, [b]gerardus.janszen@polimi.it, [c]luca.dilandro@polimi.it

Abstract

Biocomposite materials are nowadays often considered as a valid substitution of fiberglass reinforced (FGR) polymers in many relevant applications, especially thanks to the lower costs and environmental impact of the natural fibers. On the other hand, they remain mainly confined to non-structural applications. In consideration of the similar specific properties of glass and hemp fibers, the aim of this work is to compare a biocomposite component, for structural application, with a FGR-epoxy one. The comparison is focused on the issues related to the intrinsic differences of constituents mechanical characteristics as well as on their different response in the manufacturing processes. Beams with the function of wing spars, for small aeronautic structure, have been chosen as representatives. After a preliminary analysis of the materials, four spars were manufactured and were subjected to static mechanical tests up to failure, then the microstructures of failure areas were analyzed by scanning electron microscopy. The most relevant differences resulted related to the resin retention, higher in the case of the hemp fibers, to the failure modes and to the fiber-resin interactions, on which the fibers micro-structures have an important role.

Keywords

Hemp fibers, glass fibers, bio based-epoxy, structural biocomposites

Introduction

In the recent decades, natural fibers like hemp, flax, jute, and many others, have attracted the attention of many researchers and scientists as an alternative reinforcement in polymer composites. The reason lies among their advantages over conventional glass fibers: low cost, good specific mechanical properties and all the positive aspects related to their environmental impact, e.g. renewability, recyclability, bio-degradability, good availability [1-3]. Despite the interest and environmental appeal of biocomposites, their use has been limited to non-primary or low-load-bearing applications: car interior panels, furniture elements are among the present main uses of natural fibers and composites. To extend their employment fields, including light aircraft interiors and even aeronautic structural components, many researches have been recently and are presently being performed [4-7].

On the basis of fibers specific properties only, structural laminates with competitive performances compared to traditional glass reinforced composites are often expected [6]. However, the remarkably different characteristics related to the biological character of natural fiber can introduce processing drawbacks that may affect actual attainable characteristics [8,9]. For example, the hydrophilic nature of natural fibers badly combines with the hydrophobic one of many polymeric matrices; the relevant moisture absorption can impair fiber-matrix adhesion, which is a fundamental aspect for composites mechanical properties. Also, low microbial resistance and low thermal stability are problems related to natural fibers [10]. Furthermore, contrary to synthetic ones, natural fibers cannot be produced with a strictly defined and preset range of properties, since their physical and then mechanical properties depend on the starch quality, on the harvesting and extraction techniques, on the climatic conditions of the plant source site and on their specific micro-structure [11, 12]. To improve the quality of natural fibers bio composites, several techniques were developed, mainly focused on enhancing the bonding between matrix and fiber, through modification of roughness and wettability of the fibers, and on decreasing moisture absorption for better tensile properties. Alkali and acrylic acid treatments are found to be effective to modify the

fiber surface to improve the adhesion with the matrix. Also, the use of coupling agents resulted useful in this direction [10]. Thanks to these enhancements, the so called "engineered" biocomposites nowadays result suitably applicable in automotive and building industries, packaging and sports, being sometimes valid alternatives to synthetic composites of low structural performance, especially with FGR laminates [5, 13, 14].

Thermoset resins are the common basis for high performance composites. When used in natural fiber composites, they can provide higher mechanical properties with respect to the conventional thermoplastic ones, but their use makes the whole biocomposite no more biodegradable. Eco-friendly thermosets resins, with a significant content of renewable origin, are nowadays studied and developed to improve their properties towards those of synthetic origin. In this sense, the combination between natural fibers and renewable resource-based polymers can be designed to meet the demands of specific applications and simultaneously be the answer to the contemporary need [15-17]. In this view, the comparison between a synthetic composite and a biocomposite made of natural fibers and bio-epoxy resin, with structural purpose, was done in this research. Specifically, glass fibers and hemp fibers were chosen as reinforcement to be confronted, based on their comparable specific mechanical properties. Elements such as beams with the function of wing spar were chosen as representative examples of a structural component taken from aeronautic field. The aim of this research was to investigate and compare some of the actual specific issues encountered in the manufacture of the two types of composite, the mechanical characteristics in terms of bending and torsional stiffness of the final spars, their failure mechanisms and their microstructure. As a matter of facts, the very different behaviors of the two systems during manufacturing are expected to remarkably affect the final performances. By way of example, it can be predicted that the different fiber dimensions and interaction with the resins are expected to have marked influence over the fabric impregnating steps which affect the time, the extent and the overall quality of impregnation; or, again, the different fiber dimensions and properties are expected to affect failure mechanisms and therefore, to lead to remarkably different composite rupture response.

After the characterization of the base materials, the spars lay-up was designed, and four spars were manufactured. Static bending and torsional tests were performed on them before they were subjected to bending failure test. At the end, samples from the fracture area were extracted on the different spars to observe the microstructure features by scanning electron microscopy (SEM).

Experimental details

Materials

The composite spars were made by two different type of reinforcements and matrices: hemp fiber woven fabrics with green-epoxy (GE) resin on one side, and glass fiber woven fabrics with epoxy resin on the other. The main properties of the epoxy resin (Prochima, Italy, http://www.prochima.it, E-227 epoxy resin for low temperature composite lamination) and bio-epoxy resin (Sicomin, France, http://www.sicomin.com, GreenPoxy-56/ SD GP 505 V2, with about 56% matter from bio-origin), obtained from their technical datasheets, are reported in Table 1, together with the main characteristics of the fabrics. Hemp woven fabrics (0/90° plain weave, unsized, by Assocanapa, Italy, www.assocanapa.it) of 240 g/m2 (Hemp1) and 250 g/m2 (Hemp2) areal densities were used for the biocomposites, while the glass fabrics VV45 (0/90° plain weave, Glass1) and VV320T (2x2 twill weave, Glass2) (by G. Angeloni srl, Italy, www.g-angeloni.com), were used for the FGR-epoxy ones.

The number of bundles in warp and weft directions are different in the hemp fabrics, while it is equal in case of the glass fabrics. Hence, strip tests on the dry woven fabrics were carried out both in warp and weft directions, to check the response which was expected to be different in case of the hemp fabrics. This step was fundamental to correctly design the spars lay-up. An 810 MTS (Materials Test System) dynamometer was used to perform the tensile tests of hemp and glass fabrics by following the specifications given by ISO13934-1 and ASTM-D5034 standards, 50 mm wide strips were used in the tests. The hemp fabrics were dried in an oven at 80℃ for 3 hours before each measurement, test and before the lamination, to reduce the moisture content.

By means of DSC analysis both the epoxy and the bio epoxy resins were tested. A DSC 2010 Differential Scanning Calorimeter by TA Instrument was used to perform the analysis. Their glass transition temperatures were estimated on cured samples, before and after post-cure, to check the complete reaction at the end of the curing cycle followed in the spars manufacture. Temperature ramps at 10 °C/min in the temperature range of 25-170 °C (2 runs) were carried out.

A Hitachi TM3000 table-top electron microscope (SEM) was employed for microscope observations and for void content analysis. Void content was estimated from micrographs of polished sections observed at 100 X.

Spars manufacture and physical characterization

The spar structure was designed with a rectangular section and with four angle brackets going along the spar length. It was initially decided to use for all the spars the same number of layers, the same lay-up and with similar fabric areal weight, to make a comparison between the spars performances at a similar weight. To maximize the resistance to the bending moment by the angle brackets and to the torsional moment by the spar skin, the chosen lay-up was the following: $[0]_8$ for the angle brackets and $[0/45/-45]_s$ for the spar skin (the specified fibers direction is referred to that of the warp fibers). The manufacture of the spars consisted in a hand lamination and co-bonding process. The lamination was performed on an appositely designed aluminum mold, with a rectangular section of 60x120 mm, and a length of 1200, to obtain spars 1 meter long. After the cut of the angle brackets fabric layers (followed by the oven cycle for what concerns the hemp fibers), they were laminated on the rectangular mold and cured in a vacuum bag at ambient temperature. Later, they were put again on the mold and the spar skin layers were laminated above them. The whole part, then, underwent a cure cycle in the vacuum bag and a following post-cure at higher temperature, suitable for the two resins: 5 hours at 60 °C for the GreenPoxy and 3 hours at 80 °C for the epoxy E227. At the end of the curing and post-curing cycles the measured glass transition temperatures resulted Tg = 77 °C for GreenPoxy 56 and Tg = 68 °C for epoxy E227; in both cases no presence of additional reaction after post-curing was evidenced at DSC. For each spar, the fiber

fractions were estimated by weighing all the fabric used in the lamination and then the complete spars. SEM observations of either glass and hemp spar sections evidenced a quite limited presence of voids, below 2% in case of hemp laminate and below 3% in case of glass laminate (Figure 1). By knowing the resins and the fibers density, respectively ρ_m and ρ_f, the fiber volume fraction v_f was thus approximated as follows [17]:

$$v_f = \frac{\rho_m w_f}{\rho_m w_f + \rho_f w_m}. \quad (1)$$

w_f and w_m are the fiber and matrix weight fractions, respectively.

Mechanical tests

After the spar manufacture, static bending and torsion tests, with the spars in the configuration of a cantilever beam, were carried out, in consideration that these are the main loading conditions expected for a typical spar. The micro-deformation related to the load, was collected by 9 strain gauges connected to the Micro-Measurement 7000-32SM data acquisition system. An incremental tip load equal to 10 kg at each step was applied, from 0 to 40 kg. Due to the spars dimension, specific test benches were designed. The spars extremities were interfaced with the fixed support and the loading systems by means of aluminum profiles inserted into them for a length of 200 mm, and riveted to them. For the bending tests, discs of verified weight of 5 kg each, were placed on supporting plates hang to the aluminum profiles at each step. The values of the stress at each load increment, in correspondence of the strain gauges, were computed and related to the measured micro strains in those points. From these data, together with the inertia moment of the spars section, an average value of the stiffness of the different spars materials, arbitrarily approximated ~~assumed~~ as homogeneous, may be obtained. As a matter of facts, skin and angular brackets have different fiber orientations, so that actual local stresses within the spars thickness cannot be defined. Under said approximation, the value of the maximum stress σ_y under bending moment, is estimated as:

$$\sigma_{\max} = \frac{My_{\max}}{I_x}. \quad (2)$$

M is the applied bending moment, at a specific distance from the load application, on the longitudinal spar axis, y_{max} is the maximum ordinate of the spars section, which is illustrated in Figure 2, I_x is the second area moment of the cross section about the horizontal neutral axes, x.

The torsion tests were performed by modifying the apparatus used for the bending test; a pulley was fixed at the spar extremity to introduce a torque so that a pure torsional load was applied. With a procedure similar to the previous case, also the torsional stiffness of the spars was computed and the values of the maximum shear stress in correspondence of the positions of the strain gages was estimated:

$$\tau_{\max} = \frac{W}{2\Omega b_{\min}}. \quad (3)$$

W is the applied torsional moment, Ω is the surface enclosed by the midline of the section, and b_{min} is the minimum thickness of the section.

It is to be underlined that, given the natural un-homogeneities in the fibers distribution and orientation, the maximum bending stress estimated by eq. (2) and the maximum shear stress estimated by eq. (3) do not correspond to the actual maximum stresses acting in the material but have only significance for comparison.

Bending failure tests were performed to observe the failure behavior of the different composite materials. The lower values of the compression strength with respect to the tensile one, typical of the fibrous composite, suggested that the failure might occur on the side of the compressed fibers. Furthermore, some buckling phenomena were expected due to the relatively thin cross section of the spars. For these tests, a travelling crane was used as actuator to impart the load to the spar extremity. Between the crane attachment and the spar, a load cell connected to Vishay 7000-32 SM data acquisition system, with a rated capacity of 2000 kg and a rated output of 2mV/V was put to measure the applied load. The spar deflections were measured by dial indicators and a digital

potentiometer, positioned at the center span, at the fixed support and at the spar tip, respectively. The micro deformations were acquired again by strain gages. The bending failure test set-up is shown in Figure 3.

Microscopy Analysis

Glass and hemp fiber diameters were measured by SEM (Tabletop Microscope TM3000-Hitachi) images at 800 -1200 X: glass fibers are perfectly rectilinear with diameters within a narrow range of 10-12 μm; hemp fibers, instead, result twisted in the bundles and have quite irregular diameters, even along the same fiber, usually comprised in a range 13-30 μm.

At the end of mechanical tests, a SEM microscopic analysis of the composite and biocomposite spars after their breaking was performed. The fracture areas were extracted from the spars, then samples suitable for microscope observations were cut out as indicated in Figure 4. The attention was focused on the fracture areas of the different composites to study and compare the fibers conditions. In addition, several considerations about the wetting of the fibers, their structure and dimensions have been made.

Results and discussion

The characterization of base materials and the manufacture process highlighted many aspects that make the comparison of natural fiber and glass fiber composites in real applicative situations, grounded on basic properties only, quite cumbersome. Natural fiber fabrics and glass fiber fabrics have quite different densities, so the choice of similar areal reinforcement weight leads to sensibly different resulting thickness, matrix content and final weight. On the other hand, if a comparison is made on the basis of similar final weight, the remarkably different resin absorption, evidenced during manufacturing, implies that the final components again reach remarkably different fiber content. For these reasons, spars with equal main dimensions, but different thickness were produced and confronted.

Materials and composites characterization

The strip tests of dry fabrics highlighted a highly different behavior between warp and weft directions of the hemp textile (Figure 5), while the curves for glass fabric in the two directions followed almost the same path indicating a well-balanced behavior. The reason of this discrepancy for the hemp fabrics is related to a higher fiber fraction and lower crimp in the warp direction with respect to the weft one. These two characteristics provide higher stiffness and strength whereas the higher fabric crimp in the weft direction leads to higher failure strain. The average measured breaking loads per unit width of glass 1, glass 2 and hemp 1 fabrics (warp) resulted respectively 33 N/mm, 50 N/mm and 24 N/mm.

The comparison among the mechanical characteristics of the spars was initially intended to be based on a similar weight and an equal lay-up. The manufacture revealed a difficult control of the composites final weight. The hemp fabrics resulted to have a higher resin retention with respect to the glass fabrics, which resulted with a higher final resin volume fraction of the biocomposite spars. Hence, for the second fiberglass spar, a woven fabric with a higher areal weight with respect to the hemp fabrics was chosen, in the attempt to at least partially balance the final weight. In Table 2, the information on the measured composites fibers and matrix fractions and their total weight are reported.

Mechanical tests

In Figure 6 the deflection and torsion results of the different spars are reported. It is possible to observe that the measured tip deflections reached higher values in case of the two biocomposites spars notwithstanding their consistently higher thickness sections with respect to the FGR-epoxy cases.

The spars stiffness, thus, was found to be higher for the FGR-epoxy spars with respect to the biocomposites; their values are reported in Table 3, together with thickness details of the spars

parts. The measured torsion angles resulted the highest for the Glass1 spar, followed by the two hemp spars and then by the Glass 2 spar. Comparing Glass 1 and Glass 2 spars, it can be noted that, although Glass 1 has higher Vf, Glass 2 is consistently thicker, and thus stiffer. Indeed, the Glass1 spar has a value of GJ close to the one of the biocomposite spars, but its much lower thickness and weight must be considered. On a specific basis (bending stiffness/weight or torsional stiffness/weight) it can be estimated that, for the considered configurations, glass/epoxy spars are superior with a ratio of about 2-2.4 to 1 in terms of torsional or bending stiffness respect to hemp/bioepoxy elements.

During the failure test the load was increased until failure occurred. The glass reinforced composite spars showed buckling on the side subjected to compression, in proximity of the spar root. This corresponded to the expected behavior of the spar. The biocomposite spars reached the failure in a different way: no buckling phenomena were observed and the side which fractured first was the one subjected to tension in correspondence of the riveted section, at the spar root. The joint between the spar and the aluminum insert used to properly connect the spar to the fixed support failed in tension. This underlines a low resistance of the biocomposite at the riveted joint with respect to the glass-epoxy composite, and a lower tensile resistance. A following attempt to improve the riveted attachment efficiency did not lead to different failure mode. In Figure 7, the pictures of the failure area resulting from the tests are reported for the two types of composites.

Microscopy Analysis

The lower performances of the bio-epoxy resin, with respect to the E-227 epoxy, as well as the lower strength and stiffness of hemp compared to glass fabric are certainly two of the motives for the lower mechanical properties and different failure mode of natural composites. However, the lower fiber volume fraction, together with the specific structure of hemp fibers and of corresponding woven fabrics, should be ascribed as main reasons for the different response. In fact, one of the most evident difference observed with SEM analysis, resides in the bundles morphology of the two fabrics (Figure 8). While the glass fibers are well packed and aligned along the bundle longitudinal direction, the hemp elementary fibers were observed to have a certain angle with respect to the

longitudinal axis as result either of twisting during manufacture and of irregular fiber conformation. The looser packing of hemp fiber in the bundles leads to lower fiber fraction in the final laminates. In addition, the observation of the section areas showed another factor which can be considered to concur to the lower strength of biocomposites. The two types of fabrics showed a marked difference in their crimp angle: the one of the hemp fabric is very high, as consequence of the higher size of bundles. These aspects contribute to the lower tensile strength and stiffness of the hemp fabric since the fibers are remarkably misaligned with respect to applied tensile load.

As a final comment, it is to be noted that, at present, commercially available bio-based epoxy resins present thermal and mechanical characteristics comparable to common low performance epoxies; more developments are thus expected to improve their properties to meet structural applications requirements. At the same time, it should be considered that manufacturing procedure of hemp fabrics is more involved in reaching good standards in terms of appearance, handling and workability of the material rather than optimizing structural performance. It is therefore to be expected that improvement of both bio-based resins and natural reinforcements may reduce the performance gap currently present, compared to more traditional composite materials.

Conclusions

The comparison of hemp woven fabrics and glass fabrics reinforced spars showed remarkably different behavior during composite manufacturing and, consequently, in resulting structural performances. Hemp resulted in a higher retain of the resin, which might be related to the conformation and irregular packing of the fibers; this leads to lower fiber volume fractions, and lower performances with respect to the FGR-epoxy. Moreover, the remarkably different resin content increased the weight differences of the final products; the biocomposite spars resulted thicker and heavier with respect to the FGR-epoxy spars with similar plies lay-up. Static bending and torsion tests highlighted higher mechanical properties of the FGR-epoxy spars in terms of bending stiffness

and torsional stiffness. They failed under critical compressive state, while the biocomposite ones under critical tensile loads. The breaking occurred on the spars side under tension, at stresses lower with respect to the ones reached by the FGR-epoxy spars. The lower tensile strength could be ascribed to the fact that the hemp elementary fibers are not aligned with the tensile load, so that they cannot properly take proper advantage of their specific tensile performance. Microscopy analysis evidenced that they are twisted along a certain angle with respect to the longitudinal axis of the fabric bundles; the fabric crimp also contributes to a misalignment of the fibers out of the direction of the tension. The results indicate that, natural fiber/bio-based epoxy laminates can find load bearing applications, yet at the expenses of significant lower performances compared to FGR composites.

Acknowledgements

The authors wish to thank Mrs. M.R. Pagano and Eng. P. Rubini for their support in performing the tests. The work was carried out thanks to the facilities of Lab. AMALA of Politecnico di Milano.

References

1) A. Mohanty, M. Misra, L. Drzal, Journal of Polymers and the Environment, **10**, 19 (2002).

2) L. Pil, F. Bensadoun, J. Pariset, I. Verpoest, *Composites Part A: Applied Science and Manufacturing*, **4**, 193 (2016).

3) S.N. Monteiro, F.P.D. Lopes, A.S. Ferreira, D.C.O. Nascimento, *JOM*, **61**, 17 (2009).

4) R. Burgueño, M. Quagliata, A. Mohanty, G. Mehta, L. Drzal, M. Misra, *Composites Part A: Applied Science and Manufacturing*, **35**, 645 (2004).

5) C. Scarponi, *Composites Part B: Engineering*, **81**, 53 (2015).

6) O. Boegler, U. Kling, D. Empl, T. Isikveren*, Potential of sustainable materials in wing structural design*. In: Proceedings of Deutscher Luft und Raumfahrtkongress, Augsburg, September, 2014.

7) CAYLEY Project, "http://www.cayley.eu/," accessed 11.01.2018.

8) D. Puglia, F. Sarasini, C. Santulli, J.M. Kenny, *Green biocomposites: manufacturing and properties*, Chapter "Manufacturing of natural fiber/agrowaste based polymer composites", Jawaid M., Sapuan S.M., Alothman O.Y. editors, Switzerland: Springer (2017).

9) A.M. Rahman, P. Fahmida, M. Hasan, M.E. Hoque, *Manufacturing of Natural Fibre Reinforced Polymer Composites*, Chapter "Introduction to Manufacturing of Natural Fibre-Reinforced Polymer Composites", Salit M.S., Jawaid M., Yusoff N.B., Hoque M.E. editors., Switzerland: Springer (2015).

10) A. Shahzad, *Journal of Composite Materials*, **46**, 973 (2011).

11) H. Ku, H. Wang, N. Pattarachaiyakoop, M. Trada, *Composites Part B: Engineering*, **42**,856 (2011).

12) O. Faruk, A. Bledzki, H. Fink, M. Sain, *Progress in Polymer Science*, **37**, 1552 (2012).

13) B.C. Suddell, W.J. Evans, *Natural fiber, biopolymers and biocomposites*, Chapter "Natural fiber composite in automootive applications.", Mohanty A., Mishra M., Drzal L. editors., Boca Raton: CRC Press (2005).

14) M. Gupta, B. Singh, *Natural fiber, biopolymers and biocomposites*, Chapter "Natural fiber composite for building applications", Mohanty A., Mishra M., Drzal L. editors., Boca Raton: CRC Press (2005).

15) J. Rout, D. Ray, *Natural fiber, biopolymers and biocomposites*, Chapter "Thermoset biocomposites & processing of fiber plants for industral applications", Mohanty A., Mishra M., Drzal L. editors., Boca Raton: CRC Press (2005).

16) J. Summerscales, N. Dissanayake, A. Virk, W. Hall, *Composites Part A: Applied Science and Manufacturing*, **41**, 1329 (2010).

17) L. Di Landro, G. Janszen, *Composites Part B: Engineering*, **67**, 220 (2014).

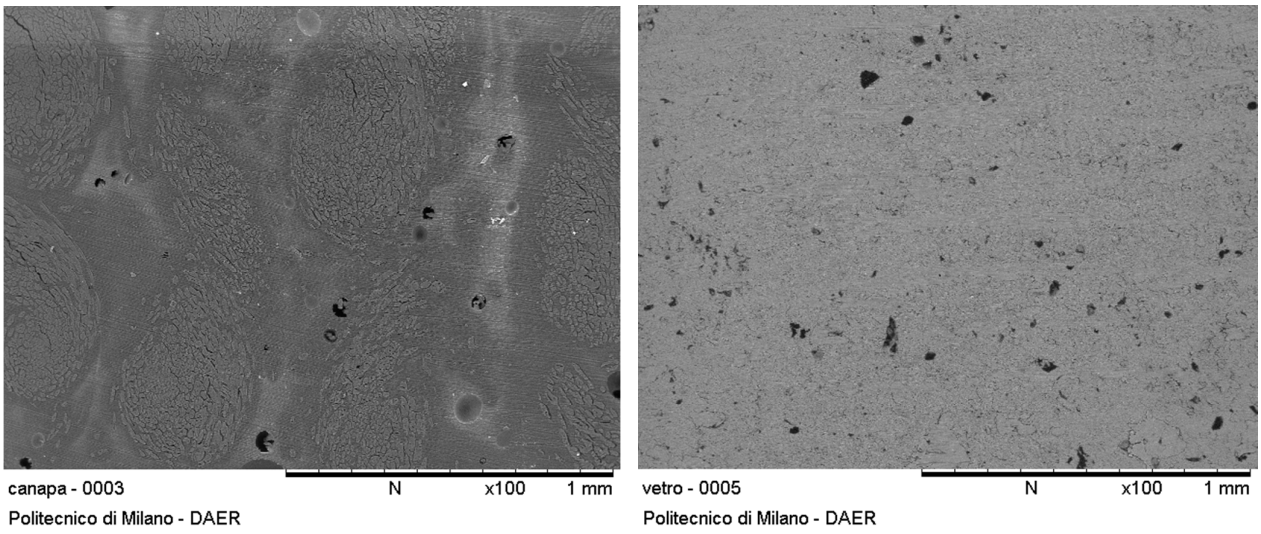

(a) (b)

Figure 1: SEM images of Hemp (a) and Glass (b) spars cross-sections for voids estimation.

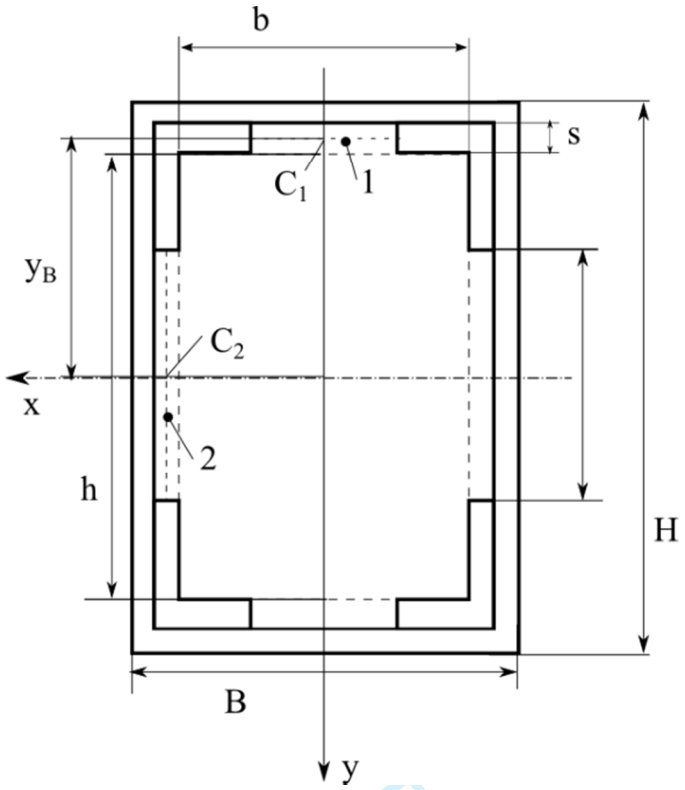

Figure 2: Spars cross section geometry.

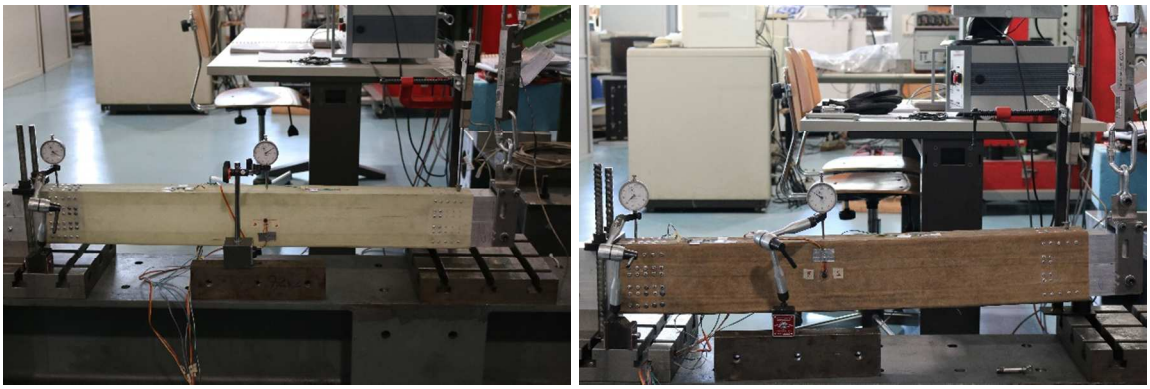

(a) (b)

Figure 3: Glass1 (a) and Hemp1 (b) composite spars during bending failure tests.

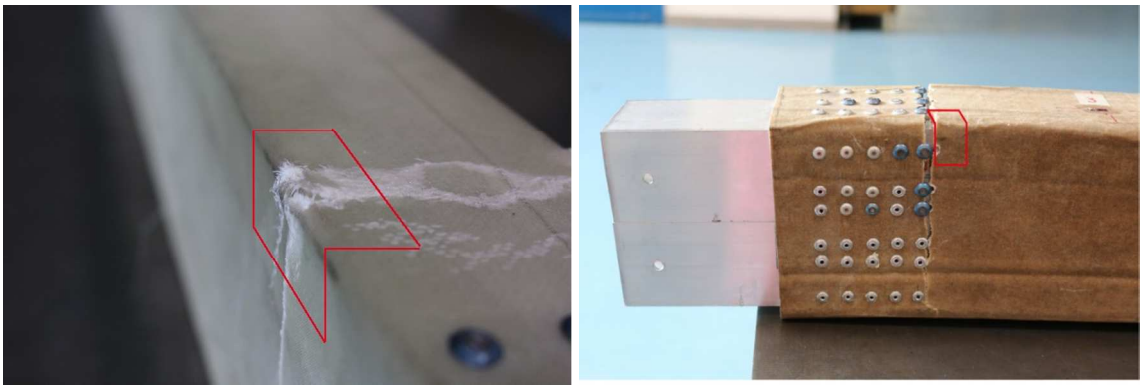

(a) (b)

Figure 4: Sample areas for SEM analysis from Glass (a) and Hemp (b) composite spars.

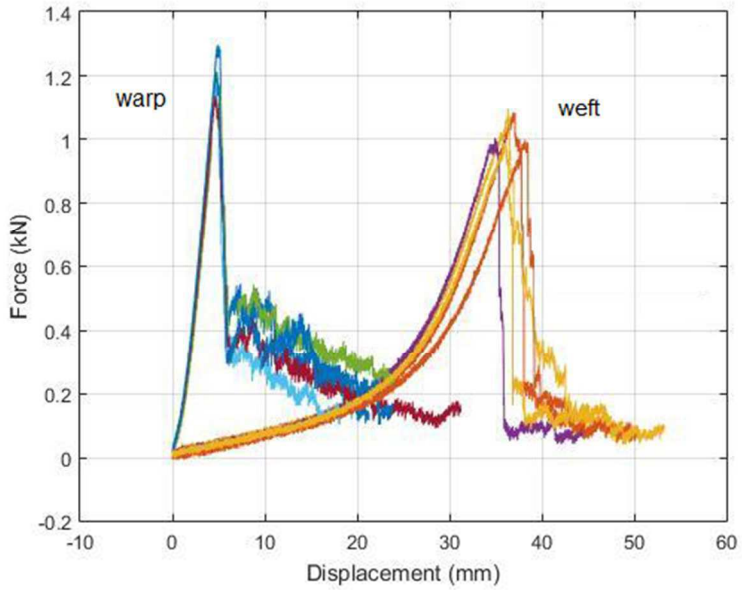

(a)

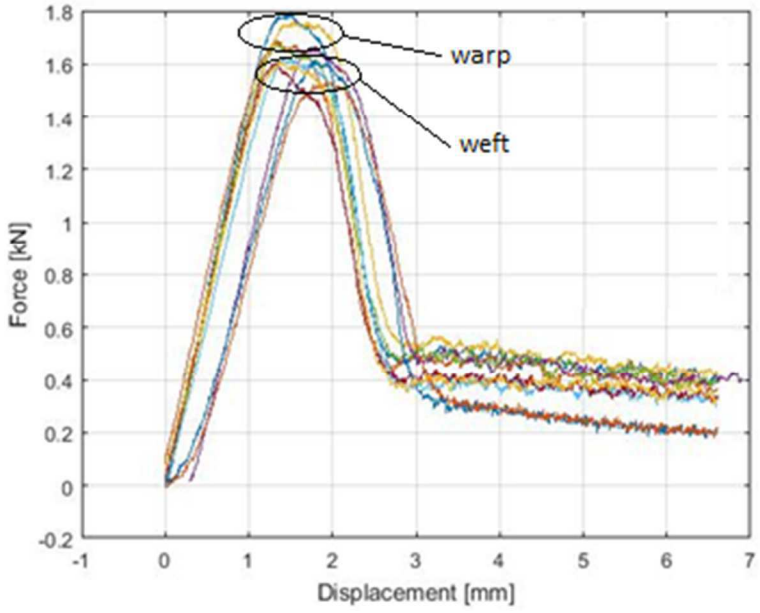

(b)

Figure 5: Strip test results for Hemp (a) and Glass (b) fabric in warp and weft directions.

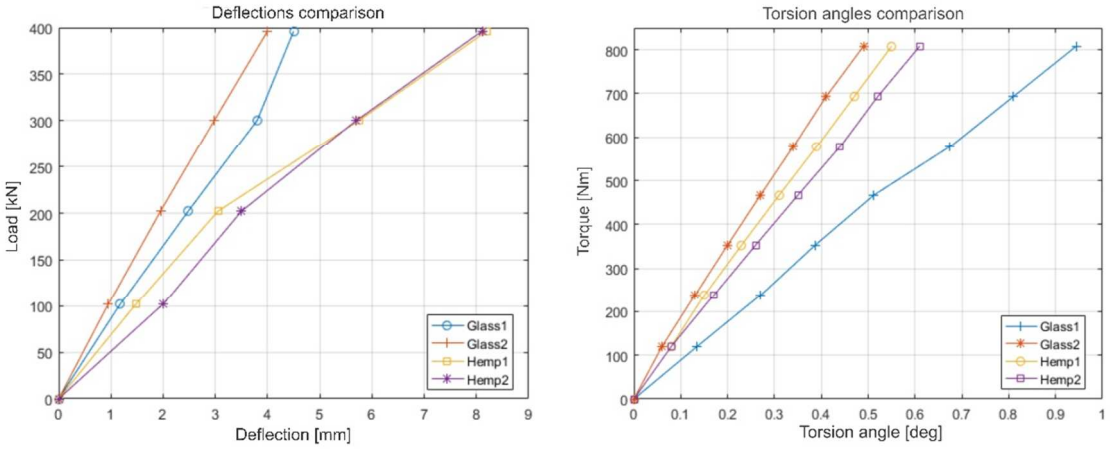

Figure 6: Deflection and torsional angle comparison of the four different spars.

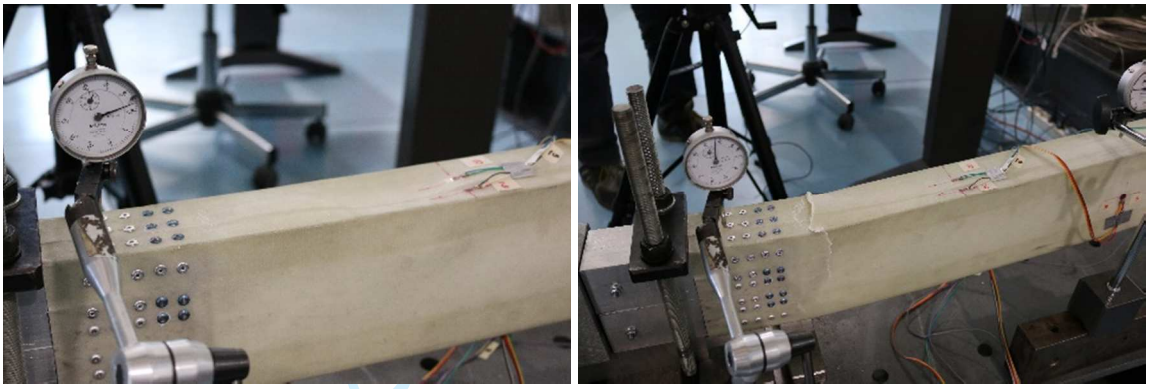

(a) (b)

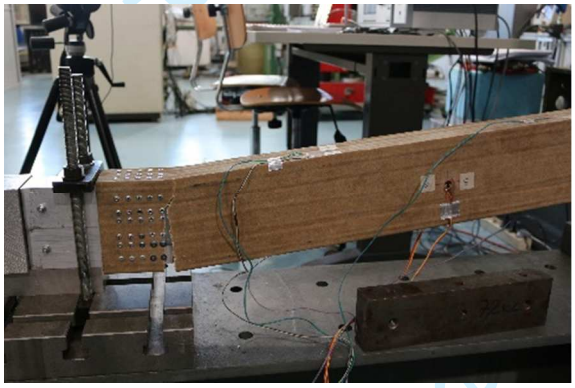

(c)

Figure 7: Images of spars during bending failure tests: buckling (a) and fracture of the Glass spar 1 (b); fracture of the Hemp spar 1 (c).

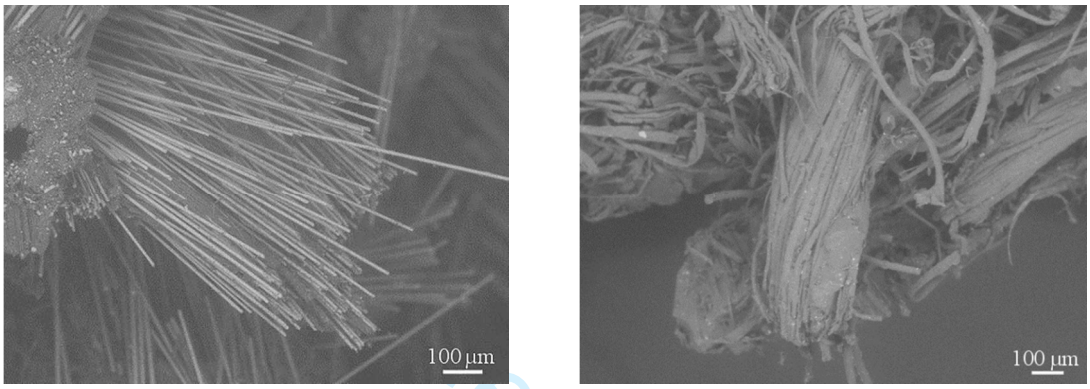

(a) (b)

Figure 8: SEM analysis: Glass (a) and Hemp bundles (b).

Table 1: Properties of employed resins and fabrics.

Material	Elastic modulus (MPa)	Tensile strength (MPa)	Viscosity (mPa.s)	Density (g/cm^3)
GE-56 (Sicomin)	3100	96	1400	1.12
E-227 (Prochima)	3500	130	1400-1500	1.19
	Fabric weave	**Areal weight (g/m^2)**	**Thickness (mm)**	**Fiber density (g/cm^3)**
Hemp1 (Assocanapa)	plain weave	240	0.54	1.45
Hemp2 (Assocanapa)	plain weave	250	0.53	1.45
Glass1 (Angeloni)	plain weave	200	0.2	2.7
Glass2 (Angeloni)	twill weave	320	0.32	2.7

Table 2: Weight and volume fractions of matrix and fiber and total weight of spars.

Spar Denomination	w_f	w_m	v_m	v_f	W_c [kg]
Hemp1	0.45	0.55	0.40	0.60	2.3
Hemp2	0.47	0.55	0.42	0.58	2.2
Glass1	0.70	0.29	0.50	0.50	1.2
Glass2	0.78	0.21	0.60	0.40	1.6

Table 3: Details of spar sections. Bending and torsional spar stiffness.

Spar denomination	Angular bracket thickness [mm]	Skin thickness [mm]	EI [kNmm^{2}x10^6]	GJ [kNmm^{2}x10^6]
Hemp1	4.3	3.4	23	12
Hemp2	4.2	3.2	26	11
Glass1	1.6	1.2	31	11
Glass2	2.5	1.8	42	20